Journal of Power Sources 267 (2014) 309–315

Contents lists available at ScienceDirect

Journal of Power Sources

journal homepage: www.elsevier.com/locate/jpowsour

Short communication

Studies on polymer nanofibre membranes with optimized core–shell structure as outstanding performance skeleton materials in gel polymer electrolytes

Haitao Bi, Gang Sui*, Xiaoping Yang

State Key Laboratory of Organic-Inorganic Composites, Beijing University of Chemical Technology, 15 Beisanhuan East Road, ChaoYang District, Beijing 100029, PR China

HIGHLIGHTS

- The skeleton materials with optimized core–shell fibre structure were prepared.
- The well-sourced polymers and facile processing techniques were involved.
- The GPE had excellent electrochemical properties and cycle performance.
- The GPE showed good stability and compatibility with lithium electrode.
- High applicable value of the GPE in lithium-ion batteries was presented.

ARTICLE INFO

Article history:
Received 26 March 2014
Received in revised form
4 May 2014
Accepted 5 May 2014
Available online 16 May 2014

Keywords:
Gel polymer electrolytes
Core–shell structure
Nanofibre membranes
Skeleton materials

ABSTRACT

The polyporous polymer nanofibre membranes with optimized core (polyacrylonitrile, PAN)-shell (polymethylmethacrylate, PMMA) structure are prepared by coaxial electrospinning, and then converted to gel polymer electrolytes (GPEs) after the activation process of stacked nanofibre membranes in liquid electrolyte. Based on the proper collocation of polymer materials, the desirable microstructure of polymer membranes as well as the affinity between fibre shell and the electrode/electrolyte result in a high saturated electrolyte uptake and conservation rate. The electrochemical testing results of the GPEs indicate high ionic conductivities, good electrochemical stability and appropriate lithium-ion transference numbers, which are realized through choosing optimal core–shell flow rate ratio. Furthermore, the interface impedance performance of the GPEs shows good stability and compatibility with lithium electrode, which is beneficial for long-term storage and use of the lithium-ion battery. The Li/GPE/$LiCoO_2$ cells with GPEs based on the electrospun membranes with optimized core–shell structure present excellent cycle performance compared to the cell involved with GPEs based on PAN and commercial Celgard 2500. Thus, the polymer membranes consisting of nanofibres with well-designed core–shell structure can be used as a new type of skeleton material in GPEs used in lithium-ion batteries.

1. Introduction

Polymer electrolytes possess relatively high ionic conductivity, as well as the unique characteristic of light weight, excellent corrosion resistance and easy shaping, have been used in chemical power sources in recent years. Many polymers, such as polyacrylonitrile (PAN), polyvinylidene fluoride (PVDF), polyethylene oxide (PEO) and polymethylmethacrylate (PMMA), etc., have been widely studied and developed as candidate materials for polymer electrolytes [1–6]. Polymer lithium-ion batteries work basically the same way as liquid lithium-ion batteries. But compared to liquid lithium-ion batteries, the energy density of polymer lithium-ion batteries is higher, and the problem of leakage of electrolyte can be avoided, followed by the enhancement of battery capacity. Polymer electrolytes can be made considerable thin and large in area to ensure fully contacts with the electrodes, facilitating development of electronic items in the direction of miniaturization, light weight and films [7]. For pragmatic reasons, polymer

* Corresponding author.
E-mail address: suigang@mail.buct.edu.cn (G. Sui).

http://dx.doi.org/10.1016/j.jpowsour.2014.05.030
0378-7753/

electrolytes must meet the following prerequisites: 1) ionic conductivity above 10^{-3} S/cm at room temperature; 2) high lithium-ion transference number; 3) electrochemical stability window is larger than 4.2 V; 4) good mechanical properties and thermal stability [8].

For now, ionic conductivity of solid polymer electrolytes is far lower than liquid electrolytes at room temperature, which limits their practical application. The different techniques, such as blending, copolymerization as well as crosslinking have been employed to fabricate polymer electrolytes with improved ionic transport properties and low crystallinity [9,10]. In addition, polymer with polyporous structure can absorb a large amount of liquid electrolytes to form gel polymer electrolytes (GPEs), so that their ionic conductivity can be close to that of liquid electrolyte. Therefore, GPEs have been widely used in the commercial polymer lithium-ion battery at present [11]. Some typical methods for the preparation of porous polymer materials include: the Bellcore process, thermally induced phase separation, thermally assisted evaporative separation, immerse precipitation, and self-assembly method [12–14]. With these methods, large amounts of organic solvents are required which can cause environmental pollution, the residue solvents can bring about negative effects on the performance. Besides, these methods are difficult to control the structure and uniformity of micropores in polymer materials. Development of electrospinning in recent years provides an effective method to prepare membranes consisting of ultrafine polymer fibres, with diameters being in the sub-micrometre down to the nanometre range [15–17]. Polymer membranes with the porosity of 30%～90% can be easily prepared by controlling electrospinning parameters. The polyporous structure can provide a large specific surface area and abundant channel for lithium ions to transfer, and improve the electrode/electrolyte interface as well as the compatibility and stability between polymer materials and liquid electrolytes. Thus, high discharge current performance and cycle performance of the obtained lithium-ion batteries can be expected.

PAN and PMMA are two cheap and well-sourced traditional electrolyte materials. PAN possesses good mechanical strength, heat resistance, chemical stability and good flame retardancy. Because some chemical actions exist between nitrile groups and lithium ions, PAN-based GPEs were reported to show bad compatibility with lithium electrodes, and the passivation on the interface can be serious [18,19]. PMMA based GPEs satisfy the needs of basic electrochemical performance, especially they have good compatibility with lithium electrode, and low interface impedance, however, the poor mechanical strength also limits their application. Blending, solvent-casting, and in situ polymerization have been attempted to form free-standing PMMA membranes with a high content of liquid electrolytes, however, it is difficult to obtain excellent electrochemical performance due to the imperfect microstructure [20]. Besides, PMMA is fragile and displays poor film-forming property during the electrospinning, continuous and uniform PMMA nanofibres are more difficult to prepare compared to PAN. In order to combine the performance advantages of different polymeric materials and polyporous structure, the polymer membranes consisting of nanofibres with core (PAN)-shell (PMMA) structure were prepared by using coaxial electrospinning in this paper. GPEs can be produced after the activation process of stacked polymer membranes in liquid electrolytes. The optimized microstructure of nanofibres and membranes was obtained by adjusting core–shell flow rate ratio, which brought the good electrochemical properties and compatibility with lithium electrode. The polymer nanofibre membranes with optimized core–shell structure can act as high performance of new skeleton material in GPEs.

2. Experimental section

2.1. Materials

PAN (average molecular weight of 10^5 g mol^{-1}, Jilin Petrochemical Co., China.), PMMA (average molecular weight of 1.2×10^5 g mol^{-1}, Aldrich Chemical Co., USA.) and *N*,*N*′-dimethylformamide (DMF, analytical reagents, Beijing Chemicals Co., China) were used to prepare the PAN and PMMA spinning solution, respectively. 1 M lithium hexafluorophosphate ($LiPF_6$)/ethylene carbonate (EC):dimethyl carbonate (DMC) (1:1, vol. %) (Battery grade, MERCK) was used as the liquid electrolyte solution.

2.2. Sample preparation

2.2.1. Preparation of polyporous polymer membranes

The polyporous polymer membranes consisting of nanofibres with core (PAN)-shell (PMMA) structure were prepared by coaxial electrospinning at room temperature and a humidity of 30%. A laboratory-produced coaxial dual-spinneret was used. A positive high voltage of 18 kV was applied to an 18-cm gap between the spinneret and a flat plate collector covered with aluminium foil. During the electrospinning process, the core–shell flow rate ratio was controlled at 0.3/0.6, 0.4/0.7, 0.8/1.0 (ml h^{-1}) by using a dual syringe pump (JZB-1800D, Jian Yuan Medical Technology Co. Ltd., China), respectively. Flow rate of shell solution was faster than that of the core solution, which could more conducive to form into continuous nanofibres with core–shell structure. The whole electrospinning process take for about 6 h. Then nanofibre membranes were vacuum-dried at 60 °C for 12 h to remove residual solvent. For comparison, electrospun PAN membranes were also prepared under the similar condition.

2.2.2. Preparation of gel polymer electrolytes (GPEs)

Polyporous polymer membranes were punched into several small discs with a diameter of 22 mm. Small discs were stacked together to form the skeleton structure of GPEs, then precursors were vacuum-dried at 50 °C for 6 h and transferred into an argon filled glove box (moisture level $<$ 10 ppm). GPEs were prepared by immersing precursors in 1 M LiPF6/EC: DMC (1:1, vol. %) for about 24 h at room temperature, the saturated GPEs were used after removal of excess liquid electrolyte with a filter paper for the measurement of electrochemical properties.

2.3. Characterization

The surface morphology of electrospun membranes was examined using scanning electron microscopy (SEM, Hitachi S-4700, Japan). The core–shell structure of single nanofibre was examined using transmission electron microscopy (TEM, Hitachi H800, Japan). *N*-butanol uptake method was employed to calculate the porosity of electrospun membranes [21].

Saturated electrolyte uptake of stacked electrospun membranes was measured after the immersion process. GPEs was placed in an argon filled glove box without sealing, and weighed every 24 h for 15 days. All the electrochemical properties were measured on Autolab PGSTAT 302N (Metrohm) at room temperature. The ionic conductivity was determined by AC impedance spectroscopy in the range of 0.1 Hz–100 KHz using the cell inserted GPEs into two parallel stainless steel (SS) discs. The electrochemical stability window was examined using the method of linear sweep voltammetry in the cell Li/GPE/SS at a scan rate of 1 mV s^{-1}, potential voltage ranging from 1 V to 7 V. The lithium-ion transference number was measured using the method of chronoamperometry (CA) in the cell Li/GPE/Li with a polarization voltage of 5 mV. The

impedance spectra were obtained by scanning in the frequency range of 0.1 Hz–200 kHz using symmetrical Li/GPE/Li cell. The total storage period was 40 days. The charge/discharge performance of the Li/GPE/$LiCoO_2$ cells was galvanostatically measured on a LAND CT2001A battery tester in the potential range of 2.7–4.2 V at current densities of 0.1 C.

3. Results and discussion

3.1. Morphological characterization of electrospun nanofibre membranes

Fig. 1 shows SEM images of coaxial electrospun membranes and TEM images of single nanofibre with a core–shell structure under different core–shell flow rate ratio. It can be seen from the SEM images that electrospun membranes possess a three-dimensional network composed by nanofibres with random orientation, resulting in a polyporous structure. Micropores in sub-microns interconnecting with each other can greatly enlarge the specific surface area, accordingly promote the adsorption capacity of liquid electrolyte. As the flow rate ratio of core–shell solution approach 1, dimension of nanofibres and micropores become more regular, average diameter of nanofibres decreased and the porosity of membranes increased. When the flow rate ratio of the core–shell solution was set as 0.8:1.0, the polymer membrane possessed a higher porosity (89%) than the other two samples (84% and 77%, respectively). Compared to the method of solution casting, phase inversion [9,22] and the commercial Celgard PE membrane [23], electrospinning showed significant advantages. Due to considerable liquid electrolyte can be absorbed through micropores, the development of abundant ionic channel can be facilitated, thus, the better electrical performance was expected. TEM images show the core–shell structure of single nanofibre in accordance with our previous report [24]. The results reveal that as the flow rate ratio of core–shell solution approach 1, thickness of the shell was decreasing while the core increased, relatively. The flow rate ratio of core–shell solution of 0.8:1.0 led to a very thin PMMA shell (24–40 nm) covered on PAN core. PAN with better mechanical performance plays an important role as the supporting phase. It also can build a transport channel for lithium ions to get through. PMMA

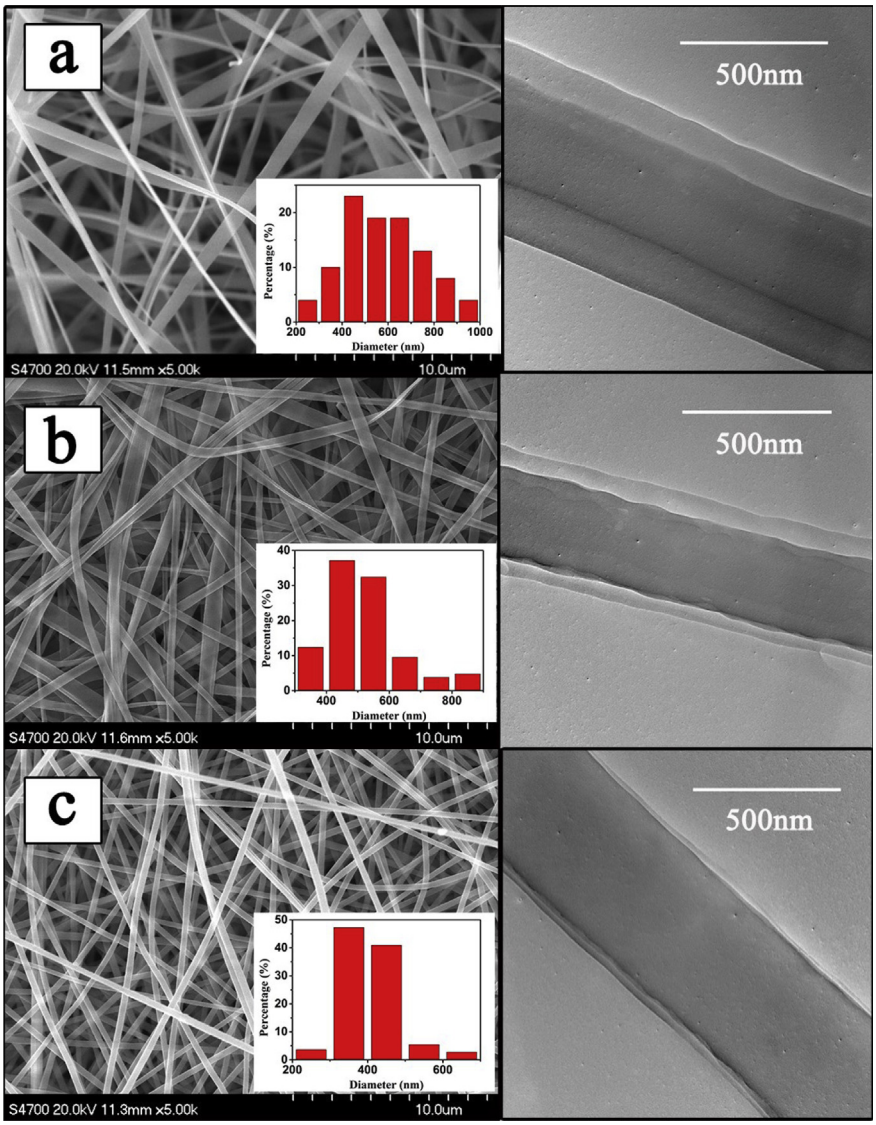

Fig. 1. SEM images (left column) of coaxial electrospun membranes and TEM images (right column) of single nanofibre with core–shell structure under different flow rate ratio of core–shell solution: (a) v_{PAN}:v_{PMMA} = 0.3:0.6; (b) v_{PAN}:v_{PMMA} = 0.4:0.7; (c) v_{PAN}:v_{PMMA} = 0.8:1.0.

covered outside the PAN phase possesses good affinity with liquid electrolyte as well as lithium electrode.

3.2. Saturated electrolyte uptake and conservation rate of electrospun nanofibre membranes

As shown in Fig. 2a, the saturated GPE based on core–shell nanofibre membranes is transparent. The saturated electrolyte uptakes (Fig. 2c) are 870%, 1006%, 1082% and 675% for stacked electrospun membranes with the core–shell flow rate ratio of 0.3:0.6, 0.4:0.7, 0.8:1.0 (ml h^{-1}), and pure PAN membranes, respectively. The uptake values are quite larger than most of the other GPEs [10,25]. Large quantities of liquid electrolyte can be absorbed by electrospun membranes in two approaches: the polyporous three-dimensional network and the partial gelation of the membranes [26–29]. Because of the poor affinity between membranes and liquid electrolytes, the gelation of pure PAN membranes is weak compared to the membranes with core–shell nanofibre structure, leading to a relatively low saturated electrolyte uptake. Owing to the good affinity of the PMMA shell with liquid electrolyte, swelling of nanofibres is distinct (Fig. 2b).

Liquid electrolyte absorbed by membranes can be lost from GPEs with time. The way of the loss mainly arised from micropores among nanofibres, liquid electrolyte in gelation form is hard to be lost. When the flow rate ratio of the core–shell solution was 0.8:1.0, the weight percentage of membrane was down to 91.6% after 15 days, higher than that of other membranes (ν_{PAN}:ν_{PMMA} = 0.4:0.7, 90.6%; ν_{PAN}:ν_{PMMA} = 0.3:0.6, 86.4%). The pure PAN membrane displayed the lowest conservation rate (84.3%). The saturated electrolyte uptake and conservation rate are closely related to the three-dimensional network, porosity, and the gelation process. Membranes obtained by coaxial electrospinning possess high saturated electrolyte uptake and conservation rate, then better electrochemical performance can be expected.

3.3. Basic measurement of electrochemical performance of the GPEs

Impedance spectra of SS/GPE/SS cells obtained in this study are shown in Fig. 3a. The ionic conductivity was calculated according to the method described in the literature [30].

The ionic conductivity of GPEs with core–shell nanofibre structure was higher than that of the pure PAN GPE (1.7×10^{-3} S cm^{-1}) [19,31]. Among them, the ionic conductivity of GPEs with core–shell flow rate ratio of 0.8:1.0 is the highest (5.1×10^{-3} S cm^{-1} vs. 4.8×10^{-3} and 4.4×10^{-3} S cm^{-1} for GPEs with core–shell flow rate ratio of 0.4:0.7 and 0.3:0.6, respectively). The high ionic conductivity is attributed to the high uptake of liquid electrolyte resulted from the fully interconnected porous structure of the membranes. Consequently, liquid electrolyte filled in the micropores and the gelation phase enriched the path for lithium ions to transport.

Linear sweep voltammogram in Fig. 3b shows that GPE of the pure PAN discomposed at about 4.5 V, while GPEs with core–shell flow rate ratio of 0.3:0.6, 0.4:0.7 and 0.8:1.0 (ml h^{-1}) discomposed

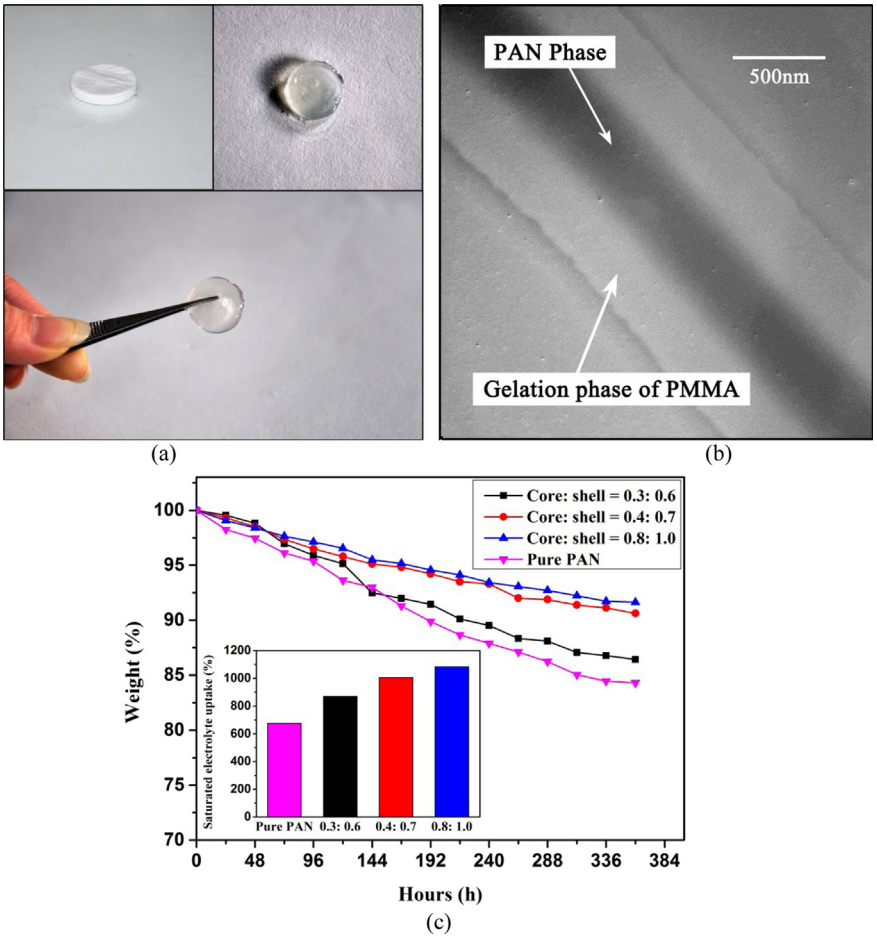

Fig. 2. (a) Morphology of the stacked nanofibre membranes and the saturated GPE; (b) TEM image of coaxial nanofibre after the gelation (ν_{PAN}:ν_{PMMA} = 0.3:0.6); (c) the change of the saturated electrolyte uptake and conservation rate with storage time.

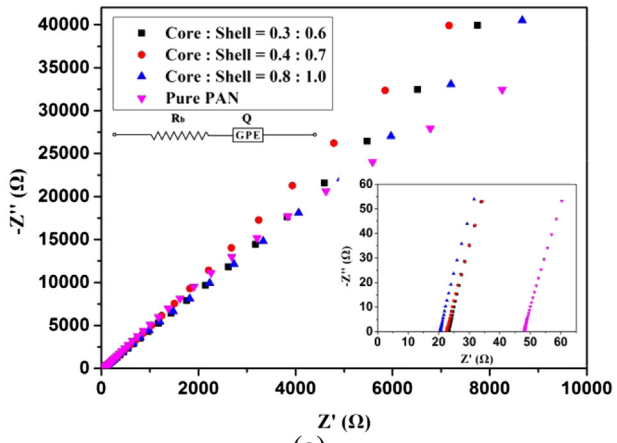

(a)

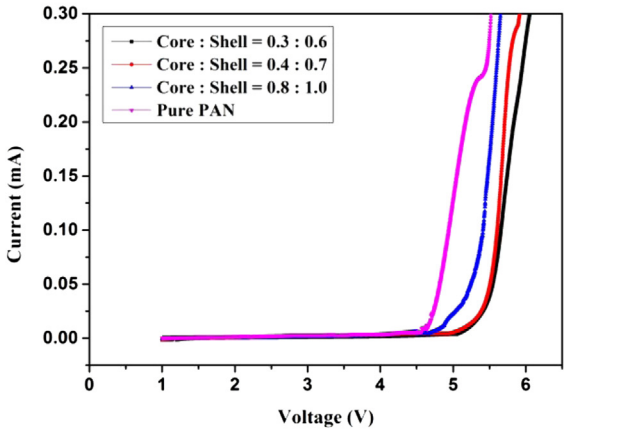

(b)

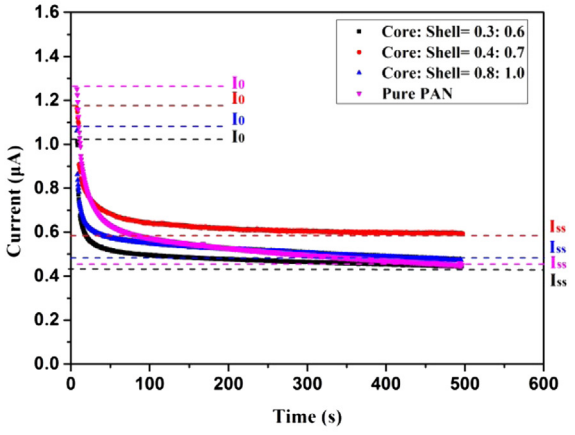

(c)

Fig. 3. Basic measurement of electrochemical performance at room temperature: (a) impedance spectra of SS/GPE/SS cells; (b) linear sweep voltammogram of Li/GPE/SS cells and (c) current response of Li/GPE/Li cells under steady state polarization.

at 5.2 V, 5.0 V and 4.7 V, respectively. Obviously, compared to the pure PAN, GPEs with core–shell nanofibre structure exhibited a better electrochemical stability. This can be ascribed to the fact that the PMMA structure can enhance the oxidation reaction to higher voltage and the excellent affinity between the ester group of PMMA and the oxygen atom of the carbonate ester group in liquid electrolyte [32,33]. Liquid electrolyte can be dissolved in the PMMA shell during the gelation process. As the flow rate ratio of the core–shell solution was close to 1, the content of PMMA was gradually reduced, and the anodic stability of GPEs decreased slightly from 5.2 V to 4.7 V.

As shown in Fig. 3c, Lithium-ion transference number (t_+) was obtained by a potentiostatic polarization method [34]. The t_+ value of pure PAN GPE was 0.41, in accordance with the reported value [35]. The t_+ value of GPEs with core–shell flow rate ratio of 0.3:0.6, 0.4:0.7, 0.8:1.0 (ml h^{-1}) was 0.46, 0.50, and 0.48, respectively. Considering the method was developed for binary and ideal solid electrolytes [36], the test error must be taken into account. Therefore, in this study, the transference number of GPEs with core–shell nanofibre structure was higher than the value of pure PAN, but showed no significant difference with the change of core–shell flow rate ratio.

3.4. Interface impedance performance of the GPEs

Based on the analysis hereinbefore, GPEs with core–shell flow rate ratio of 0.8:1.0 were chosen during the interface impedance performance test. The initial interface impedance spectra of Li/GPE/Li cells containing core–shell structure or pure PAN nanofibre membranes are presented in Fig. 4a, semi circles in the high frequency region and straight lines in the low frequency region are observed just as the other typical electrolytes [37]. The values of bulk electrolyte resistance (R_b) and interfacial resistance (R_i) can be obtained from the equivalent circuit diagrams from the experimental impedance spectra. The evolution of R_b and R_i of Li/GPE/Li cells with two kinds of GPEs are shown in Fig. 4b. The values of R_b are related to the nature of GPEs, which showed no significant difference with the storage time, while the values of R_i underwent

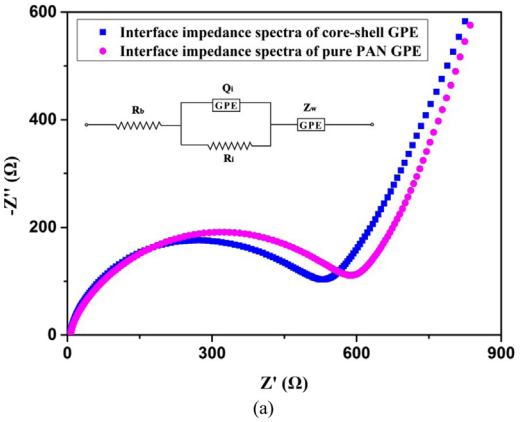

(a)

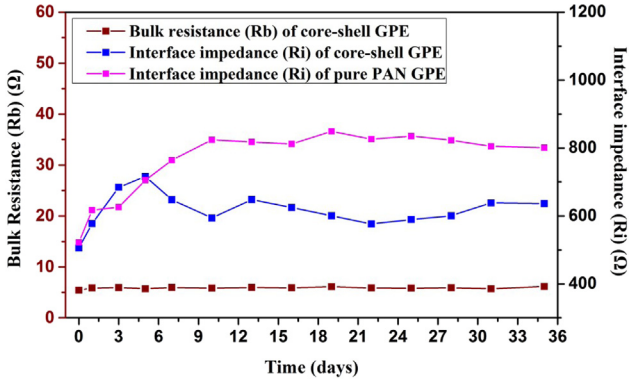

(b)

Fig. 4. (a) Initial interface impedance spectra of Li/GPE/Li cells based on core–shell; (b) pure PAN nanofibre membranes, and evolution of R_b and R_i with storage time.

obvious changes. It can be seen that R_i of the GPE based on core–shell nanofibre membranes increased rapidly in the first five days up to 720 Ω, followed by a decrease, vibrating in a small range around the level of 600 Ω as the gelation progressed. While R_i of the GPE based on pure PAN membranes show a sustained increase up to a higher level. The evolution of R_i is closely related to the interface stability between electrodes and electrolytes, which can affect the cyclic stability and rate capacity of lithium-ion battery [38–40]. The above results indicated that the GPE based on core–shell nanofibre membranes had better stability and compatibility with lithium electrode than that of the GPE based on pure PAN membranes.

3.5. Cycle performance of the Li/GPE/$LiCoO_2$ cells

Fig. 5a shows the initial discharge capacities of the Li/GPE/$LiCoO_2$ cells using different electrolytes at 0.1 C rate at room temperature. The cell with the GPE based on electrospun membranes with the flow rate ratio of core–shell solution of 0.8:1.0 delivers an initial discharge capacity of 135 mAh g^{-1}, which is 95.1% of the theoretical capacity of $LiCoO_2$ (142 mAh g^{-1}) and larger than the cell with GPEs based on PAN (130 mAh g^{-1}) and Celgard 2500 (126 mAh g^{-1}).

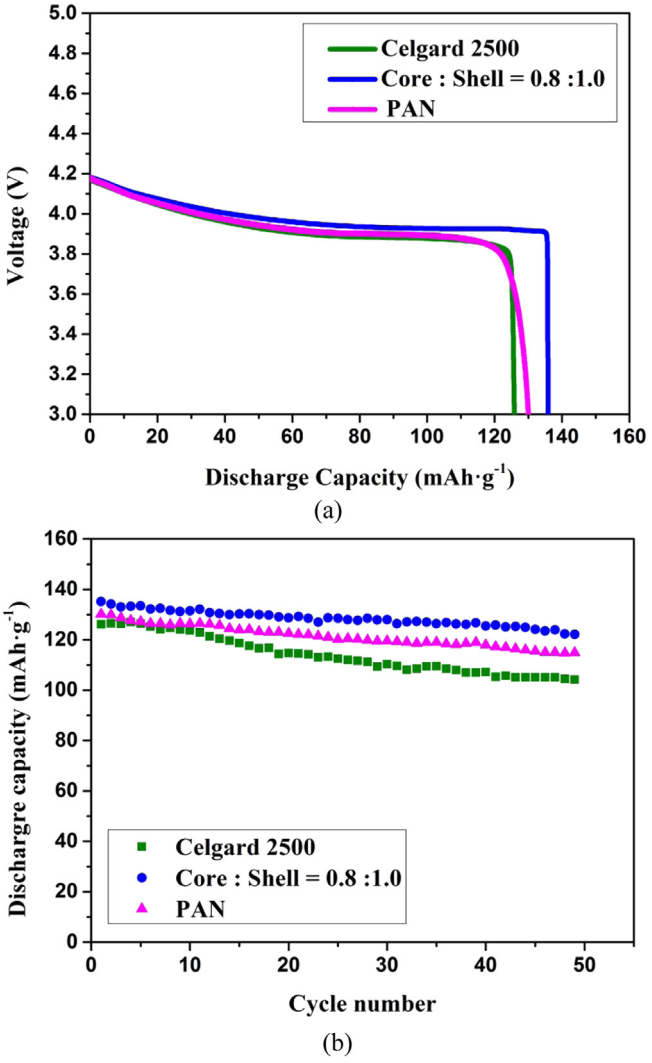

Fig. 5. (a) Initial discharge properties of Li/GPE/$LiCoO_2$ cells using different electrolytes (25 °C, 0.1 C, 2.75–4.2 V); (b) The cyclic stability of the Li/GPE/$LiCoO_2$ cells using different electrolytes up to 50 cycles (25 °C, 0.1 C, 2.7–4.2 V).

Fig. 5b shows the cyclic stability of the Li/GPE/$LiCoO_2$ cells with GPEs based on the electrospun membranes with the flow rate ratio of core–shell solution of 0.8:1.0, PAN and Celgard 2500 membranes up to 50 cycles (25 °C, 0.1 C, 2.7–4.2 V). It can be seen that the cell with GPEs based on electrospun membranes with the flow rate ratio of core–shell solution of 0.8:1.0 has higher primary capacity and better cyclic stability than the cell with PAN. After 50 cycles the cell with GPEs based on electrospun membranes with the flow rate ratio of core–shell solution of 0.8:1.0 retains 90.4% of its initial discharge capacity, while the cell with GPEs based on PAN retains only 87.7% of its initial capacity. For a comparison, the cell using Celgard 2500 under identical conditions shows poorer cyclic stability, which remains only 82.6% of its initial capacity after 50 cycles. The excellent cycle performance of GPEs based on electrospun membranes with optimized core–shell structure attributes to the following two aspects: 1) excellent ionic conductivity induced by abundant ionic channels, high saturated electrolyte uptake and conservation rate, originated from fully interconnected micropores; 2) excellent interface impedance performance induced by the core–shell structure, which can provide stability and compatibility between nanofibres and lithium electrodes/liquid electrolyte.

4. Conclusions

The polymer nanofibre membranes with core (PAN)-shell (PMMA) structure were prepared by using coaxial electrospinning under different flow rate ratio of the core–shell solution. The microstructure of nanofibres and membranes could be controlled by changing the flow rate ratio of core–shell solution during electrospinning. Non-woven nanofibre membranes were activated in liquid electrolyte after being stacked together to form into GPEs. High saturated electrolyte uptake and conservation rate were observed for the stacked polymer nanofibre membranes, which led to a remarkable electrochemical performance. Based on the optimization of core–shell flow rate ratio, high ionic conductivities, electrochemical stability and lithium-ion transference numbers of the resulting GPEs were obtained. Moreover, the GPEs showed good interface stability and compatibility with lithium electrode. Core (PAN)–shell (PMMA) based GPEs showed excellent initial discharge capacities as well as remarkable cycle performance ascribed to high porosity, remarkable electrochemical performance and excellent interface impedance performance. Through the implementation of the proper collocation of two well-sourced polymer materials and facile preparation techniques, comprehensive performance of the resulting GPEs is more superior to that of the commercial Celgard products. Consequently, the polymer nanofibre membranes with well-designed core–shell fibre structure will be an ideal skeleton material in GPEs used in lithium-ion batteries with high performance.

Acknowledgement

This research was supported by National Natural Science Foundation of China (No. 51073019), the Program for New Century Excellent Talents in University (No. NCET-12-0761) and the National High-tech R&D Program of China (863 Program) (No. 2012AA03A203).

References

[1] C.Y. Chiang, M. Jaipal Reddy, P.P. Chu, Solid State Ionics 175 (2004) 631.
[2] V. Gentili, S. Panero, P. Reale, B. Scrosati, J. Power Sources 170 (2007) 185.

[3] D. Peramunage, D.M. Pasquariello, K.M. Abraham, J. Electrochem. Soc. 142 (1995) 1789.
[4] H.R. Allcock, M.E. Napierala, D.L. Olmeijer, C.G. Cameron, S.E. Kuharcik, C.S. Reed, S.J. O'Connor, Electrochim. Acta 43 (1998) 1145.
[5] Y.H. Liao, D.Y. Zhou, M.M. Rao, W.S. Li, Z.P. Cai, Y. Liang, C.L. Tan, J. Power Sources 189 (2009) 139.
[6] A.I. Gopalan, P. Santhosh, K.M. Manesh, J.H. Nho, S.H. Kim, C.G. Hwang, K.P. Lee, J. Membr. Sci. 325 (2008) 683.
[7] J.Y. Song, Y.Y. Wang, C.C. Wan, J. Power Sources 77 (1999) 183.
[8] K. Murata, S. Izuchi, Y. Yoshihisa, Electrochim. Acta 45 (2000) 1501.
[9] M.M. Rao, J.S. Liu, W.S. Li, Y. Liang, D.Y. Zhou, J. Membr. Sci. 322 (2008) 314.
[10] M. Rao, X. Geng, Y. Liao, S. Hu, W. Li, J. Membr. Sci. 399 (2012) 37.
[11] K. Kezuka, T. Hatazawa, K. Nakajima, J. Power Sources 97 (2001) 755.
[12] A.S. Gozdz, C.N. Schmutz, J.M.Tarascon, P.C. Warren, US Patent, 5418091, 1995.
[13] H. Huang, S.L. Wunder, J. Electrochem. Soc. 148 (2001) A279.
[14] T. Michot, A. Nishimoto, M. Watanabe, Electrochim. Acta 45 (2000) 1347.
[15] D.H. Reneker, I. Chun, Nanotechnology 7 (1996) 216.
[16] Y.A. Dzenis, Science 304 (2004) 1917.
[17] A. Greiner, J.H. Wendorff, Angew. Chem. Int. Ed. 46 (2007) 5670.
[18] K.H. Lee, J.K. Park, W.J. Kim, Electrochim. Acta 45 (2000) 1301.
[19] H.J. Ryoo, H.T. Kim, Y.G. Lee, J.K. Park, S.I. Moon, J. Solid State Electrochem. 3 (1998) 1.
[20] H. Fan, H. Li, L.Z. Fan, Q. Shi, J. Power Sources 249 (2014) 392.
[21] S.W. Choi, J.R. Kim, S.M. Jo, W.S. Lee, Y.R. Kim, J. Electrochem. Soc. 152 (2005) 989.
[22] M.M. Rao, J.S. Liu, W.S. Li, Y. Liang, D.Y. Zhou, J. Power Sources 184 (2008) 477.
[23] S.W. Choi, S.M. Jo, W.S. Lee, Y.R. Kim, Adv. Mater. 15 (2003) 2027.
[24] S. Lin, Q. Cai, J. Ji, G. Sui, Y. Yu, X.P. Yang, X. Deng, Compos. Sci. Technol. 68 (2008) 3322.
[25] H.R. Jung, W.J. Lee, Electrochim. Acta 58 (2011) 674.
[26] P. Raghavan, X. Zhao, C. Shin, D.H. Baek, J.W. Choi, J. Manuel, C. Nah, J. Power Sources 195 (2010) 6088.
[27] Q. Xiao, Z. Li, D. Gao, H. Zhang, J. Membr. Sci. 326 (2009) 260.
[28] J.R. Kim, S.W. Choi, S.M. Jo, W.S. Lee, B.C. Kim, Electrochim. Acta 50 (2004) 69.
[29] A.M.M. Ali, M.Z.A. Yahya, H. Bahron, R.H.Y. Subban, M.K. Harun, I. Atan, Mater. Lett. 61 (2007) 2026.
[30] G.B. Appetecchi, F. Croce, B. Scrosati, J. Power Sources 66 (1997) 77.
[31] P. Raghavan, J. Manuel, X. Zhao, D.S. Kim, J.H. Ahn, C. Nah, J. Power Sources 196 (2011) 6742.
[32] S.J. Gwon, J.H. Choi, J.Y. Sohn, Y.E. Ihm, Y.C. Nho, Nucl. Instrum. Meth. Phys. Res. Sect. B 267 (2009) 3309.
[33] D. Ostrovskii, A. Brodin, L.M. Torell, G.B. Appetecchi, B. Scrosati, J. Chem. Phys. 109 (1998) 7618.
[34] J. Evans, C.A. Vincent, P.G. Bruce, Polymer 28 (1987) 2324.
[35] G. Feuillade, P. Perche, J. Appl. Electrochem 5 (1975) 63.
[36] P.G. Bruce, C.A. Vincent, J. Electroanal. Chem. 225 (1987) 1.
[37] E. Barsoukov, J.R. Macdonald (Eds.), Wiley-Interscience, 2005.
[38] Y.G. Lee, J.K. Park, S.I. Moon, Electrochim. Acta 46 (2000) 533.
[39] N. Chaix, F. Alloin, J.P. Bélières, J. Saunier, J.Y. Sanchez, Electrochim. Acta 47 (2002) 1327.
[40] N.S. Choi, Y.M. Lee, J.H. Park, J.K. Park, J. Power Sources 119 (2003) 610.